J. Plasma Physics (2010), *vol.* 76, *parts* 3&4, *pp.* 355–367.
doi:10.1017/S0022377809990626

Some surprising manifestations of charged particle dynamics in a magnetic field

RAM K. VARMA

Physical Research Laboratory, Ahmedabad 380 009, India
(ramkvarma@gmail.com)

(Received 15 November 2009 and accepted 8 December 2009, first published online 15 January 2010)

Abstract. We present here some very unusual experimental results on the dynamics of charged particle in a magnetic field which cannot be comprehended in terms of the Lorentz dynamics regarded, as per the current conceptual framework, as the appropriate one for the macro-scale description. Astonishingly, these results have been shown to be manifestations of a novel macro-scale quantum structure, designated as 'transition amplitude wave' (TAW), riding with the guiding centre trajectory, which is generated in the latter trajectory in consequence of the scattering of the particle with a fixed scattering centre. One set of observed results is thus identified as matter wave interference effects on the macro-scale attributable to this entity. The other enigmatic observation demonstrates the detection of a curl-free magnetic vector potential on the macro-scale, which is also shown to be a consequence of the TAW embedded in the Lorentz trajectory. These enigmatic results thus point to the unravelling of a new concept of a 'dressed' Lorentz trajectory—dressed with the TAW—accountable for these results, as against the 'bare' trajectory. These results and the formalism which enables one to comprehend them have led to the emergence of a new class of phenomena which display quantum properties on the macro-scale.

1. Introduction

The dynamics of charged particles in a magnetic field have been studied for over a century and its properties have been central to the studies in relation to fusion and space plasmas as well as numerous other applications pertaining to beam optics with the Lorentz equation as the governing equation. Our studies have, however, unravelled certain features of the motion on the macro-scale which, paradoxically, cannot be comprehended in terms of the Lorentz equation to whose domain the motion ostensibly pertains. We have observed some fascinating features which are unexpected and unsuspected from the viewpoint of the conventional understanding.

In what follows we first describe the enigmatic experimental results alluded to above pointing out how unsuspectingly different they are from the ones expected *à* la the classical Lorentz equation of motion in the context of the particular system studied. Next, we describe their characteristics and later present the new theoretical framework in terms of which these results could be understood. In fact, it is the theoretical formalism which had predicted the effects which were subsequently substantiated by these experimental results. It is pointed out that the theoretical formalism has introduced an entirely new concept, not hitherto

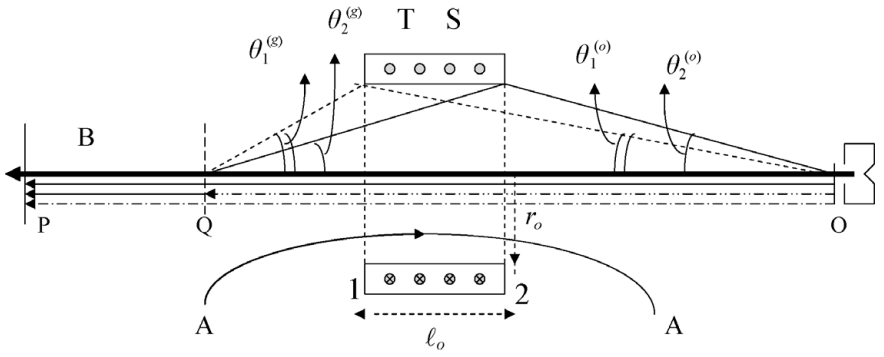

Figure 1. Schematic representation of the experimental arrangement, with the toroidal solenoid TS (length ℓ_o, radius r_o), the position of the plate P, of the electron gun O and the position of the grid Q. The various angles $\theta_1^{(g)}$, $\theta_2^{(g)}$, $\theta_1^{(o)}$ and $\theta_2^{(o)}$ are as shown. Bold line with an arrow from O to P represents the magnetic field. Full lines from O to P and from Q to P denote the propagation lines of the 'transition amplitude wave', while the dash-dotted broken lines from O to P and O to Q represent the propagation lines of the de Broglie waves along the magnetic field. The curved line AA represents a typical field line of the curl-free vector potential produced by the toroidal solenoid TS.

advanced, which has manifested in these enigmatic results. This concept has evolved over the years through both theoretical [1–6] and experimental [7–9] investigations. However, it must be pointed out that these results, notwithstanding their heterodox nature, are not violative of the Lorentz equation. In fact, as shown later, the new dynamical concepts relating to these effects are external to the purview of the Lorentz dynamics as we understand it and therefore do not violate it. This may sound puzzling, but will be clarified later.

2. Description of the experiments

We begin by presenting a sequence of experiments which exhibit the unusual behaviour alluded to above. The experiments are extremely simple, easily repeatable and the results obtained are robust. The simplest of these experiments consists in studying the behaviour of an electron beam of extremely low current ($\sim nA$) injected along an almost homogeneous magnetic field in a highly evacuated vacuum glass chamber ($\sim 5 \times 10^{-7}$ torr) with a very small pitch angle ($<5°$). The electron gun is situated at one end of the glass chamber with a collector plate situated at the other end about 50 cm away. In addition, a movable grid is situated between the electron gun and the collector plate.

The high vacuum of the chamber is meant to ensure that a e-neutral collision mean free path is very much longer than the dimensions of the chamber, while the low beam current ensures that the electrons behave essentially as individual particles, ruling out entirely the possibility of collective behaviour This is an extremely important requirement. The experimental system is schematically shown in Fig. 1

2.1. Electron energy sweep with the grid close to the collector plate

The experiment is carried out by fixing the magnetic field at a certain appropriate value and recording the plate as well as grid currents (with both of them grounded)

https://doi.org/10.1017/S0022377809990626 Published online by Cambridge University Press

as the electron beam energy is swept over a range ∼10 eV–1 keV. One could use the Lorentz dynamics to predict the possible plate current response as the electron beam energy is swept. It would appear reasonable to expect that the plate current response would be monotonic with a monotonic sweep of the electron energy: rising from a small value and saturating to a plateau—something like as shown in Fig. 2(a). However, the actually observed plate current response in the above experiment, as shown in Fig. 2(b), is astonishingly at variance from the expected monotonic one.

The plate current exhibits an undulatory response which is entirely unexpected. Significantly, the grid current response anti-correlates entirely with the plate current response. Clearly, such a behaviour cannot be understood in terms of the Lorentz equation of motion. It has been argued in detail in [7] that any collective effects or plasma instability must be ruled out as an origin of this effect. Moreover, these results have been successfully reproduced by other workers [10] as well, and they have also been scrutinized for their inexplainability in terms of a model based on the Lorentz dynamics [10, 11].

If we convert the plate current profile of Fig. 2(b) into a plot against $\mathscr{E}^{-1/2}$ in place of the original one against the energy $\mathscr{E}$ expressed in volts, we obtain the profile as given in Fig. 2(c). Interestingly, this profile displays peaks that are equidistant (in terms of the variable $\mathscr{E}^{-1/2}$). This behaviour points to a regularity which is an important signature of this effect and will be seen to have a bearing on its nature. It has also been observed [8] that the 'frequency' of these oscillations (with respect to $\mathscr{E}^{-1/2}$) increases with both the increase of the magnetic field B and the increase in the gun–plate distance L_p. Both these dependencies would again seen to be entirely unsuspected. Figure 2(d), which depicts a Fourier plot of the curve of Fig. 2(c), exhibits a dominant peak corresponding to the periodic peaks in this figure. There also exist smaller harmonic peaks with twice and thrice the (fundamental) frequency.

We next present the results of yet another experiment which is small but important variation of the earlier one. Thereafter, we shall present an outline of the theoretical formalism relating to it.

2.2. Electron energy sweep with a finite distance between the grid and the plate

The experiment is carried out as before, but now with the grid placed at a finite distance away from the plate (6 cm). With the gun–plate distance fixed as before, and the external magnetic field tuned to a certain appropriate value, the electron energy is swept over the same range as before. Both the plate and grid currents (both grounded) against the energy $\mathscr{E}$ (in Volts) as recorded in the experiment are shown in Fig. 3(a). When plotted against $\mathscr{E}^{-1/2}$ as before, these are given in Fig. 3(b). This figure displays two interesting features: (i) There exist equidistant peaks as before in Fig. 2(c). Besides, there exist also envelopes (with equidistant nodes and anti-nodes) over these peaks which have the appearance of 'beats'. That these are really wave 'beats' as in the case of sound or other waves will be seen below. Here again, the plate and grid currents anti-correlate entirely, and Fig. 3(c), which depicts the Fourier plot of the curves of Fig. 3(b), exhibits two dominant close frequency peaks that account for the generation of the beats shown in Fig. 3(b). In the Fourier plot of Fig. 3(c), a small frequency peak is also seen, which is equal to the difference between the two dominant frequencies. This peak obviously represents the beat frequency. It proves that the envelopes exhibited in Fig. 3(b) do indeed

https://doi.org/10.1017/S0022377809990626 Published online by Cambridge University Press

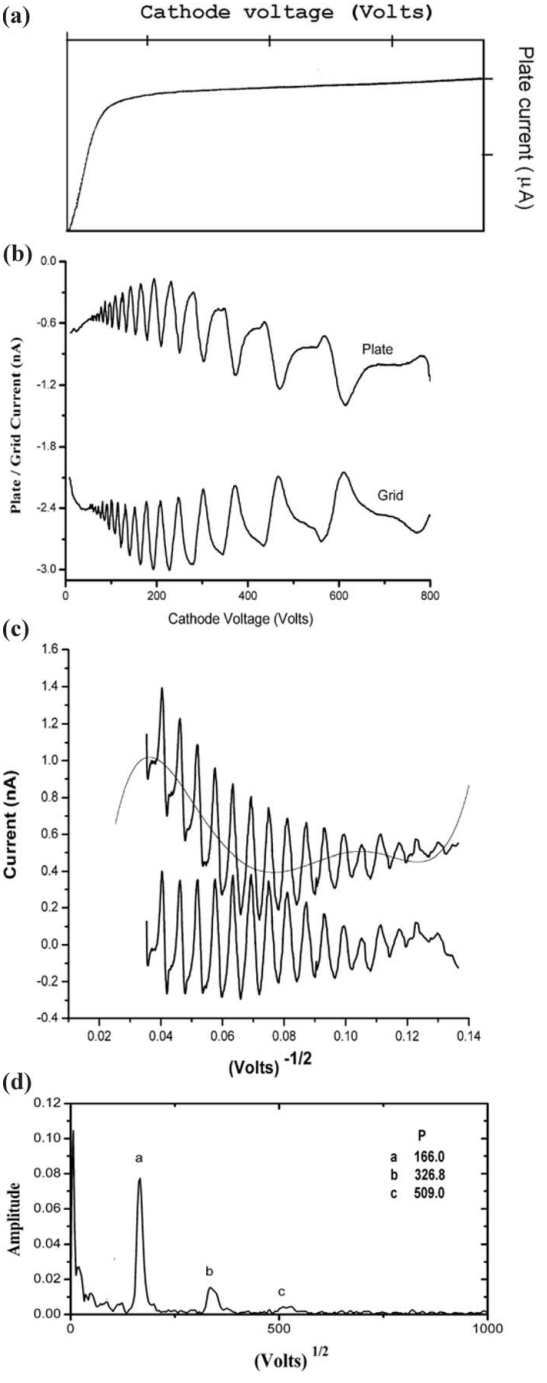

Figure 2. Plate/grid current variation with the electron energy sweep with, gun–plate distance $L_p = 51$ cm and magnetic field $B = 69$ G. (a) Monotonic response of plate current with the monotonic sweep of electron energy $\mathscr{E}$ as expected according to Lorentz dynamics. (b) Actually observed plate and grid current responses. (c) Plate current response of (b) replotted as a function of $\mathscr{E}^{-1/2}$.(d) Fourier plot of curves of (c), showing a dominant frequency peak and two non-dominant peaks corresponding to the second and third harmonics.

https://doi.org/10.1017/S0022377809990626 Published online by Cambridge University Press

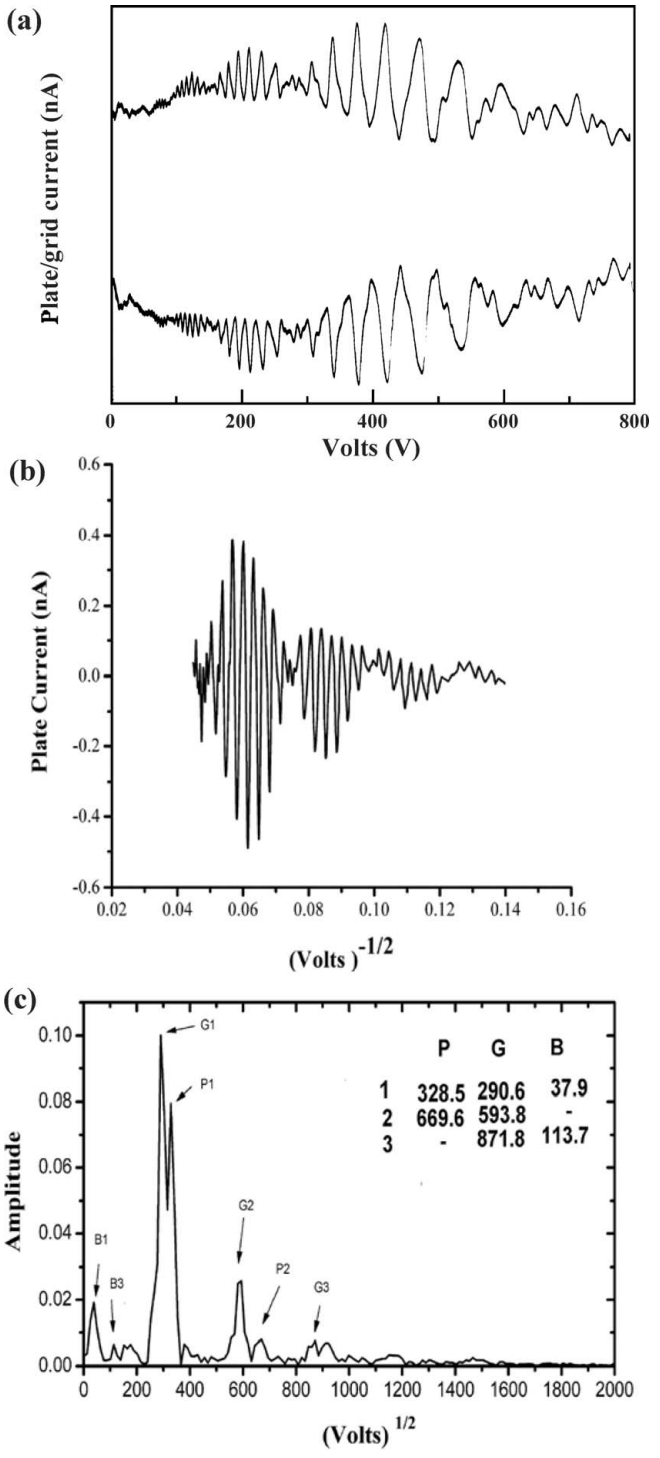

Figure 3. Plate/grid current variation with electron energy sweep, with grid-plate distance $D = (L_p - L_g) = 6$ cm, $L_p = 51$ cm and magnetic field $B = 135G$. (a) The plate current as a function of energy $\mathscr{E}$; (b) plate current of (a) transformed in terms of $\mathscr{E}^{-1/2}$; (c) Fourier plot for the curve of (b).

https://doi.org/10.1017/S0022377809990626 Published online by Cambridge University Press

depict beats between the two 'frequencies' determined by the two distances in the experiment—the gun–plate distance L_p and the gun–grid distance L_g with the beat frequency determined by the difference $(L_p - L_g)$. Thus, the undulating response of the plate (and grid) current can be attributed to a wave nature of the dynamical system.

What is noteworthy about the plot of Fig. 3(b) as contrasted with that of Fig. 2(c) is that the qualitative difference between the two arises only because of the different positions of the grid in the two cases. In fact, as shown in [9], a systematic variation of the grid position away from the plate has resulted in the corresponding plate current profiles to be qualitatively different from the preceding ones. This should itself come as a surprise in an experimental set-up such as this one, because according to the Lorentz dynamics, a grounded grid intervening the plate and the electron gun is not supposed to make any essential difference to the charged particle flow from the gun to the plate, *regardless of its position*. It is clear that contrary to the common perception, the grounded grid in this experiment is playing a non-trivial role. The nature of the role that the grid position plays will become shortly apparent.

3. Towards understanding these phenomena

As indicated above, an understanding of these results entails the use of an entirely new matter wave concept associated with a magnetized charged particle, which has evolved through a formalism developed in [2, 3, 5]. We present below a physical picture of the idea that this formalism expresses in a formal language.

Consider a charged particle in the magnetic field suffering a collision with a fixed centre. As a consequence, it would, in general, exchange energies between its parallel and perpendicular degrees of freedom. According to classical mechanics, the energy exchange has a continuous spectrum; it can vary from one collision to another in a continuous manner. However, quantum mechanically, the exchange can occur only in terms of an integral number of discrete quanta of energy of magnitude $\hbar\Omega$ where $\Omega = eB/mc$ is the electron gyro-frequency and $\hbar\Omega$ is inter-Landau level spacing. It will be seen that, interestingly, it is this characteristic that leads to the concept referred to above, and which ultimately accounts for the observed enigmatic behaviour. In other words, strange as it may appear, the effects that are observed to be on the macro-scale are really of quantum origin.

Let $\mathscr{E}$ be the total particle energy which can be written as $\mathscr{E} = (\hbar k)^2/2m + (N + 1/2)\hbar\Omega$, where $\hbar k$ is the particle momentum along the field and $(N + 1/2)\hbar\Omega$ is the quantized perpendicular energy of the Landau state of quantum number $N \gg 1$. The scattering of the particle against a fixed centre conserves the total particle energy in the collision. If (N', k') is the post-scattering quantities, then one has

$$\frac{(\hbar k)^2}{2m} + N\hbar\Omega = \frac{(\hbar k')^2}{2m} + N'\hbar\omega. \tag{3.1}$$

Writing $N' = N + n$, $(n \ll N, N \gg 1)$ and $n\kappa = k - k'$, one has (taking $k' \sim k$)

$$k - k' = n\kappa = n\Omega/v, \tag{3.2}$$

where we have written $\hbar(k + k') \simeq 2\hbar k = 2mv$, v being the particle parallel velocity, then (3.1) and (3.2) may be written in the form

$$E = E' + n\hbar\Omega, \quad P = P' + n\hbar\Omega/v, \tag{3.3}$$

https://doi.org/10.1017/S0022377809990626 Published online by Cambridge University Press

where P and P' are the parallel momenta $P = \hbar k$ and $P' = \hbar k'$. Equation (3.3) may be regarded as 'energy-momentum' conservation relation for the guiding centre motion pre- and post-scattering

$$(E, P) = (E', P') + n(\epsilon, \varpi), \tag{3.4}$$

where $\epsilon = \hbar\Omega$ and $\varpi = \hbar\kappa$, and (ϵ, ϖ) may be regarded as an energy-momentum packet that may be considered to be exchanged in the process of scattering. Note also that $\epsilon = \varpi v$ (or equivalently $\Omega = \kappa v$) represents a 'dispersion relation' which shows that the packet (ϵ, ϖ) moves with the particle's guiding centre. This packet may thus be regarded as a 'quasi-particle' generated in the guiding centre trajectory as a consequence of transition across Landau levels in the process of scattering. This would be a unique kind of 'quasi-particle' which rides 'piggyback' on the guiding centre motion. Clearly, this is a consequence of the discrete nature of the Landau levels and hence of quantum origin. One can associate a matter wave with this 'quasi-particle' with a wavelength given by $\lambda_{qp} = 2\pi/\kappa = 2\pi v/\Omega$.

The above simple treatment provides a physical interpretation of the formalism [3,5] which embeds this concept in a more formal language. The matter wavelength λ_{qp} given above has been identified to belong to the matter wave designated as 'transition amplitude wave' (TAW). This concept has, in fact, been developed formally in [5] with the above expression of the wavelength, $\lambda_{qp} = 2\pi v/\Omega$, having been explicitly derived in [5]. It is now claimed that the observed results actually represent matter wave interference effects (in one dimension) on the macro-scale which are attributable to the 'transition amplitude wave'. What would appear rather astonishing to the reader is that the above matter wavelength has an $\hbar$-independent expression and that (as a consequence) it falls on the macro-scale. For typical laboratory parameters, electron energy $\mathscr{E} \simeq 1$ keV, and magnetic field $B = 100$ G, $\lambda_{qp} \sim 5$ cm, a large wave length for a matter wave indeed! (A detailed discussion of the macro-scale nature of this wave with the above wavelength is given in [6].) Furthermore, as demonstrated below, it has indeed manifested in the experiments as represented in Figs 2 and 3. The $\hbar$-independence of the wavelength is a unique characteristic of this matter wave which is an entirely new concept, and distinct from the de Broglie wave. That this matter wave should yet be within the framework of quantum mechanics may sound somewhat puzzling. The formalism of [3, 5] indeed demonstrates the manner in which this concept flows from the quantum formalism in response to some specific questions. This is what makes this concept so fascinating.

3.1. The experimental results as macro-scale matter wave interference effects

We now briefly present an algorithm for the explanation of the results depicted in Figs 2 and 3 as one-dimensional interference effects with the macro-scale matter wavelength $\lambda_{qp} = 2\pi v/\Omega$ (wavenumber $\kappa = \Omega/v$). We refer to Fig. 1 to describe the algorithm. Recall that the TAW is generated in consequence of a scattering suffered by the particle against a centre as it transits from the gun to the plate. We identify different points where scattering can occur and the TAWs generated. (i) One is the grid Q at $x = x_g$ against whose wires the particle can be scattered either by image charges or by direct grazing encounters. (ii) Second, the anode region of the gun O at $x = x_o$ which has a 'perpendicular' component of the accelerating electric field. This 'perpendicular' field will also kick particles across Landau levels. The propagation lines of the TAW are shown by solid lines emanating from the

https://doi.org/10.1017/S0022377809990626 Published online by Cambridge University Press

respective sources. On the other hand, before the scattering they propagate as de Broglie waves shown by broken lines in the figure.

The wave amplitudes of the TAW reaching the plate P at x_p from these sources are given by

$$\Psi_{(0,1,2)} = A_{(0,1,2)} \exp\left[i\kappa(x_p - x_{(p,0,g)})\right], \tag{3.5}$$

where this equation represents the two TAW amplitudes reaching the plate with different suffixes $(1,2)$, corresponding respectively to TAWs emanating from the gun at O at the position x_o and the grid Q at the position x_g with amplitudes being A_1 and A_2. In addition, a third amplitude A_0 is also included which corresponds to the unscattered de Broglie wave, which is represented in (3.6) by a propagation of the TAW from x_p to x_p. This last one essentially corresponds to the unscattered de Broglie wave amplitude (which can be looked at as a TAW travelling from x_p to x_p, which must be included in the total TAW amplitudes reaching the plate). The total wave (TAW) amplitude reaching the plate is given by

$$\Psi(x_p) = e^{i\kappa x_p}\left[A_0 e^{-i\kappa x_p} + A_1 e^{-ix_o} + A_2 e^{-ix_g}\right]. \tag{3.6}$$

Evaluating the probability density $|\Psi(x_p)|^2$ for the $\Psi(x_p)$ given by (3.6) yields an expression which is analyzed in [4, 8] for the different cases corresponding to Figs 2 and 3. Figures 2(b) and (c) correspond to the case that the grid is close to the plate Q, so that one has $D(= L_p - L_g = x_p - x_g) \lll L_p(= x_p - x_o)$. Under these conditions, the probability density at the plate $|\Psi_p|^2$ is given by

$$|\Psi_p|^2 = C_1 + C_2 \cos\kappa L_p + C_3 \cos 2\kappa L_p, \tag{3.7}$$

where C_1, C_2, C_3 are given in terms of the coefficients in (3.6); these are detailed in [4, 8]. This expression describes a periodic variation of the plate current with the variation of $\kappa = (m/2)^{1/2}(\Omega/\mathscr{E}^{1/2}) \sim \mathscr{E}^{-1/2}$. This is precisely what is seen in the experimental curves of Figs 2(b) and (c). The frequency f of the undulations represented by (3.7) is given by $f = (m/2)^{1/2}\Omega L_p$. Such a dependence has indeed been verified in the experiments [8, 9]. It has been demonstrated that the inter-peak separation decreases inversely with both B and L in accordance with the above expression for the frequency f.

We next consider the case $(L_p - L_g) \leq \epsilon L_p$ (with $\epsilon \leq 0.2$). This corresponds to the case of Figs 3(a) and (b). For this case, we have the expression (as worked out in [8, 11])

$$|\Psi_p|^2 = c_1 + C_2 \cos\kappa L_p + C_3 \cos 2\kappa L_p - C_4 \sin^2 \frac{1}{2}\kappa(L_p - L_g)\cos\kappa L_p \tag{3.8}$$

with an expression for C_4 as given in [11]. The last term in (3.8) describes an oscillation represented by $\cos\kappa L_p$ modulated by the 'beat' frequency $\Omega(L_p - L_g)$. This is essentially what is demonstrated in Fig. 3(b) with the observed beat frequency being described by this term. This confirms that the observed beats are essentially wave beats that have been described by the above wave algorithm. Furthermore, the beat frequency, according to the above expression, increases with the increase of the separation $D = L_p - L_g$. This has been seen in the experiments reported in [9].

https://doi.org/10.1017/S0022377809990626 Published online by Cambridge University Press

4. Observation of curl-free vector potential on the macro-scale

We next describe an even more spectacular effect, namely the observation on the macro-scale of a curl-free vector potential. This would be considered quite exceptional because, as mentioned above, in the canonical picture where Lorentz dynamics is the descriptor of macro-scale processes, a curl-free vector potential cannot have an observable effect. We shall briefly describe the formalism which predicts the above effect and later describe the experimental results demonstrating it. The equation of evolution of the TAW which predicts this effect is given by [3]

$$\frac{i\mu}{n}\frac{\partial\Psi(n)}{\partial t} = \frac{1}{2m}\left(\frac{\mu}{in}\frac{\partial}{\partial x} - \frac{e}{c}A_x\right)^2 \Psi(n) + \mu\Omega\Psi(n), \tag{4.1}$$

where $\mu = (\frac{1}{2}mv_\perp^2/\Omega = N\hbar)$ is the gyro-action for the perpendicular motion which also equals $N\hbar$, the action associated with the Nth Landau level $N \simeq 10^8$. A_x is the x component of a curl-free vector potential

Note that (4.1) is, interestingly, of the Schrödinger form (one-dimensional), which involves the vector potential in the same manner as in the quantic Schrodinger equation (except for the large action $\mu = N\hbar$ in place of $\hbar$) with n having the same meaning as in (3.3). Because of the presence of A_x in (4.1), it predicts the observation of the curl-free vector potential on the macro-scale and, moreover, in one-dimension. A detailed discussion of its observability is given in a recent paper [6]. The observability of the vector potential is effected, as in the Aharonov–Bohm case, through a 'fringe shift' of the interference maxima of the TAW, described in Sec. 3 and depicted in Fig. 2

Now we describe the algorithm based on (4.1) to bring out the manner in which the above-mentioned observation of the curl-free vector potential can be effected. We refer to the experimental system in Fig. 1, which is essentially the same as described in Sec. 3. In addition, we have a toroidally wound solenoid (TS) which produces the curl-free vector potential in the space around, because such a solenoid would ideally have the magnetic flux completely trapped inside it. The TAW is generated as before at the position of the electron gun O at x_o, and by the grid Q at $x = x_g$, as electron beam propagates from these to the plate through the space now permeated by the vector potential. From (4.1) one has the wave amplitudes $\Psi^{(n)}_{(1,2)}$ for propagation from x_o and x_g given by (with appropriately suffixed indices)

$$\Psi^{(n)}_{(1,2)} = A^{(n)}_{(1,2)} \exp\left[\frac{ni}{\mu}\int_{(x_o,x_g)}^{x_p} dx'\left(mv + \frac{e}{c}A_x\right)\right]. \tag{4.2}$$

where one has used the form $\Psi^{n)} \sim \exp[ni\mathscr{E}t/\mu]$ for the stationary state and introduced $v = [2(\mathscr{E}-\mu\Omega)/m]^{1/2}$ as the parallel velocity. The total probability amplitude reaching the plate is given by $\Psi = \Psi_1 + \Psi_2$, and the probability density $|\Psi(x_p)|^2$is evaluated (specializing to $n = 1$). This is then integrated over a distribution in μ, $g(\mu) = (\beta/\sqrt{\pi})\exp[-\beta^2(\mu-\bar{\mu})^2]$, arising from a spread in pitch angle injection. The resulting expression for the probability density is given by

$$\left\langle|\Psi(x_p)|^2\right\rangle = {A_1}^2 + {A_2}^2 + 2A_1A_2F(X)\cos\left[\frac{1}{\bar{\mu}}\int_{x_o}^{x_g} dx'\left(m\bar{v} + \frac{e}{c}A_x\right)\right] \tag{4.3}$$

https://doi.org/10.1017/S0022377809990626 Published online by Cambridge University Press

with $F(X)$ given by $F(X) = \exp[-(X/2\beta\bar{\mu})^2]$ and X given by

$$X \equiv \int_{x_O}^{x_g} (\Omega/v)\, dx' - 2\pi k. \tag{4.4}$$

The implication of (4.3) along with (4.4) is that (a) the amplitude $F(X)$ of the cosine factor in (4.3) is maximum for $X = 0$, and (b) the cosine factor itself yields a number of maxima for

$$\int_{x_o}^{x_g} \left(m\bar{v} + \frac{e}{c}A_x\right) dx' = 2\pi\ell\bar{\mu},\ \ell = 1, 2, 3, \ldots. \tag{4.5}$$

It can be shown that $\int_{x_o}^{x_g} A_x dx' = G\Phi$, where Φ is the total flux trapped in the toroid, and G is a geometrical factor $G < 1$. We note that the condition $X = 0$, which is essentially the same condition ($\kappa L(p, g) = 2\pi k,\ k = 1, 2, 3, \ldots,$) defining the interference maxima of Fig. 2, locates the interference maximum and maximizes the amplitude of the cosine term in (4.3). In the experiment, such a maximum can be obtained by tuning the magnetic field with the electron beam of a certain energy $\mathscr{E}$ on, and a given gun–grid distance $L_g = (x_g - x_o)$. The condition (4.5), on the other hand, would be satisfied by varying the vector potential field in space. This will lead to the periodic variation of the probability current at the collector plate as represented by $\langle|\Psi_p|^2\rangle$ of (4.3). This thus provides the manner of detection of the vector potential as the flux in the toroid producing the latter is varied by varying the current feeding it. Because the curl-free vector potential cannot affect the particle velocity $\bar{v}$ in (4.5), it is sufficient to write (4.5) in terms of the differences $\Delta\int_{x_o}^{x_g} A_x dx' = G\Delta\Phi$ and $\Delta\ell$. One thus has the condition

$$\Delta\Phi = \frac{c}{e}2\pi\bar{\mu}(\Delta\ell), \Delta\ell = 1, 2, 3, \ldots \tag{4.6}$$

for the maxima of the cosine function.

As Φ varies, the interference maximum defined by $X = 0 \rightarrow \Omega L_g = 2\pi v$ (first interference maximum, for $k = 1$) returns for $\Delta\ell = 1, 2, 3, \ldots$. The condition $\Omega L_g = 2\pi v$ can be incorporated in (4.6) by dividing the latter by the former, yielding

$$\Delta I = \frac{c}{2e}\frac{mv_o L_p}{\Gamma G}\left(\frac{B_p}{B_o}\right)\sin\delta\tan\delta(\Delta\ell), \ldots, \Delta\ell = 1, 2, 3, \ldots, \tag{4.7}$$

where we have written $\bar{\mu} = \mathscr{E}\sin^2\delta/\Omega$, δ being the pitch angle of injection, and $\Delta\Phi = \Gamma(\Delta I)$, I being the current feeding the toroidal solenoid with Γ containing information about the permeability of the solenoid core and its dimensions.

Relation (4.7) predicts the observability of the effect of curl-free vector potential through the observation of a sequence of maxima for $\Delta\ell = 1, 2, 3$, as the current in the solenoid is swept. It predicts the dependence of the inter-peak interval $\Delta^{(1)}I$ (for $\Delta\ell = 1$) on the velocity $v_o \sim \mathscr{E}^{1/2}$. Besides this, there is also a dependence on the geometrical factor G. The experiment has been carried out as outlined above. Figure 4 gives the variation of the plate current as the solenoidal current I is varied for the various energies $\mathscr{E} = 600$, 800, 1000, 1100, 1200 eV.

If the vector potential were not to affect the dynamics of the charged particles, then the plate current should exhibit a 'flat' response as a function of the toroid current. The plot (left-hand panel of Fig. 4), on the other hand, shows a strong undulatory (periodic) response (with an amplitude ∼50%). In the right-hand panel of Fig. 4 are Fourier plots of the corresponding curves in the left-hand panel. The

https://doi.org/10.1017/S0022377809990626 Published online by Cambridge University Press

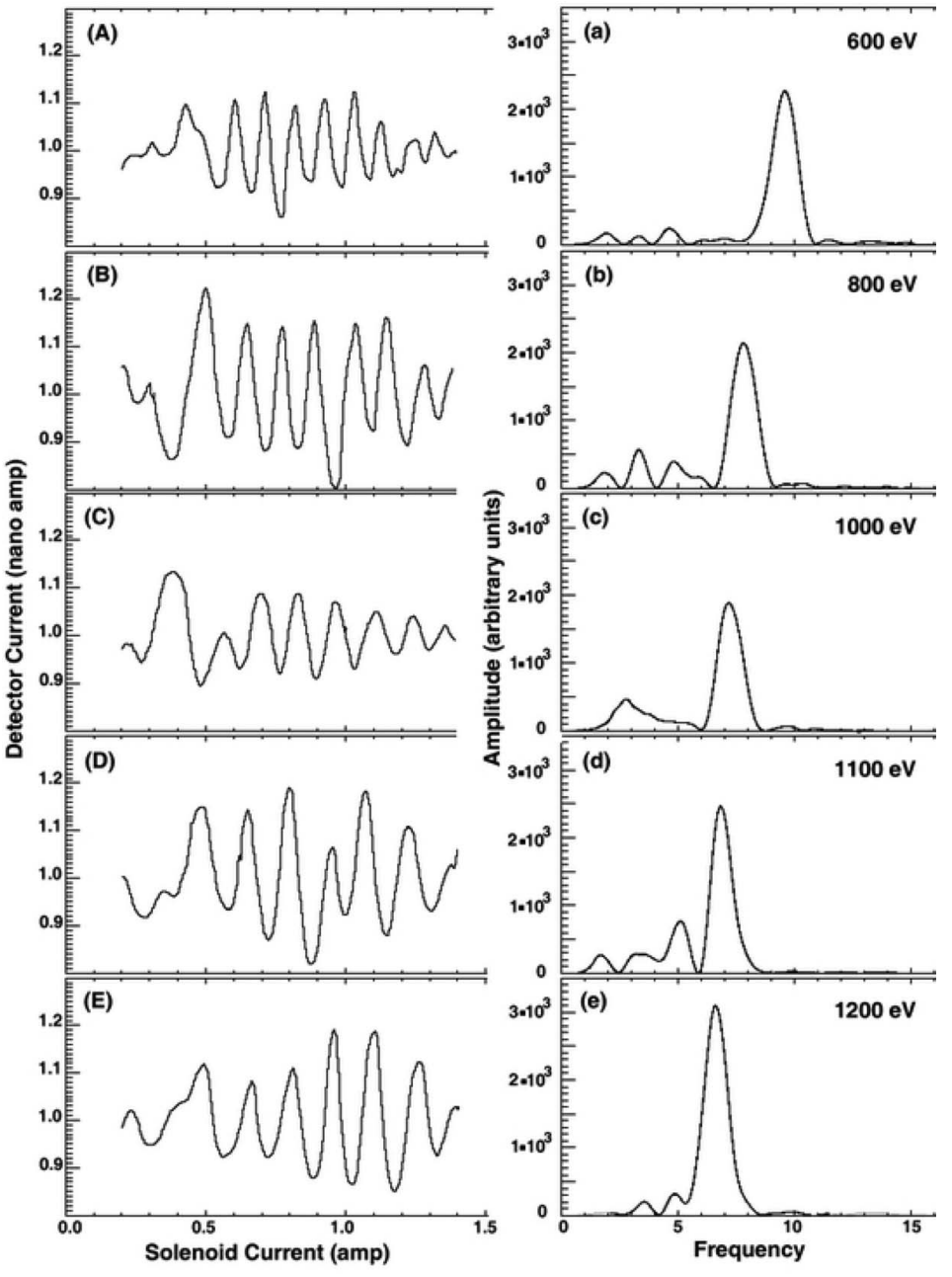

Figure 4. Detector plate current against the current in the toroidal solenoid. (A)–(E) Detector current in nA against the solenoidal current in amperes (A), for the electron energies $\mathscr{E}$(eV) = 600, 800, 1000, 1100 and 1200. These have been corrected for the saturating core which leads to dilation in the inter-peak separation in the original plots with increasing solenoidal current. (a)–(e) The Fourier plots corresponding to (A)–(E).

https://doi.org/10.1017/S0022377809990626 Published online by Cambridge University Press

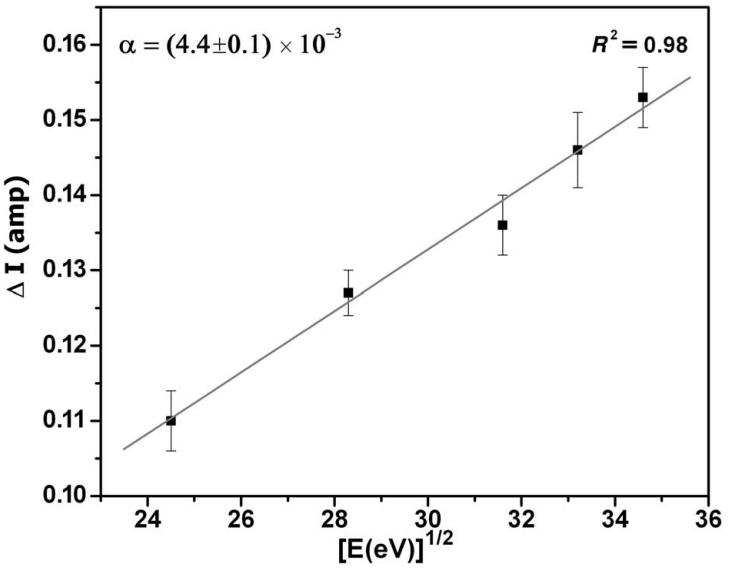

Figure 5. Dependence of ΔI on $\mathscr{E}^{-1/2}$; α denotes the slope of the straight line fit in the figure.

dominant Fourier peaks in these plots represent frequencies, the inverse of which would give the inter-peak separation ΔI as defined by the relation (4.7). Figure 5 exhibits the dependence of ΔI so determined on the electron energy going as $\sqrt{\mathscr{E}}$, which is predicted by the relation (4.7). The degree of correlation is quite high with $R^2 = 0.98$. The observations described above thus demonstrate the detection of the curl-free vector in conformity with the prediction of the formalism of [3, 5]. There is an additional very interesting dependence of the inter-peak separation ΔI on the plate grid distance $D = L_p - L_g$, whose consequences have been worked out in detail in [6]. For brevity, we do not dwell on this issue.

5. Concluding comments

It would appear quite astonishing that the dynamical system of charged particles in a magnetic field which has been studied so extensively over the years should reveal such a novel behaviour on the macro-scale which has been missed so far. Clearly, none of the two class of experiments which obviously pertain to the macro-scale could be comprehended in terms of the Lorentz dynamics in whose domain they fall. The more striking of these is the observation on the macro-scale of the effect of a curl-free vector potential that the Lorentz equation does not even recognize. Obviously, there is a new physics at play underlying these enigmatic phenomena. As shown above, the new physics involves, quite astonishingly, the interplay of the quantum structure of the trajectory in a rather novel fashion, leading to the new concept—the 'transition amplitude wave' (TAW) which characterizes the behaviour on the macro-scale.

Thus, the results reported here have not only unravelled entirely unexpected new features of charged particle dynamics in a magnetic field but also led to the formulation of an entirely new quantum concept—the TAW, not hitherto recognized,

https://doi.org/10.1017/S0022377809990626 Published online by Cambridge University Press

which relates to macro-scale phenomena as against the conventional association of quantum dynamics with micro-scale phenomena.

Notwithstanding their enigmatic nature and the inadequacy of Lorentz dynamics to explain them, these results do not imply a violation of the Lorentz equation but rather the presence of the macro-scale quantum entity—the TAW embedded in the Lorentz trajectory, so that both the attributes—the TAW and the Lorentz dynamics—co-exist. This is a rather unique situation not hitherto encountered. One may describe this state figuratively as a Lorentz trajectory being 'dressed' with the 'transition amplitude wave' and attribute the observed effects to the 'dressed trajectory', in particular, its 'dress'. The 'dress' itself is created through transition across Landau levels. But the Lorentz trajectory itself is little affected by the 'dress'. One can use the term 'bare' Lorentz trajectory to describe the trajectory without the dress. The bare trajectory is what is determined by the Lorentz equation and the existence of 'dressed' trajectory does not violate the latter. One may refer to [6] for a detailed discussion on this point.

A tribute

It is a great pleasure to submit this paper for the special volume of the *Journal* in honour of Padma Shukla on the occasion of his sixtieth birthday. I have chosen to present in this paper some ideas that have been dear to me, which I have followed over approximately the same number of years as I have known Padma. My association with Padma since 1975, when I first met him in Lausanne, has been both extremely delightful and fruitful both personally and professionally. I wish Padma many more creative, healthy and happy years ahead, as the ones gone by.

References

[1] Varma, R. K. 1971 *Phys. Rev. Lett* **26**, 417.
[2] Varma, R. K. 1985 *Phys. Rev.* A **31**, 3951.
[3] Varma, R. K. 2001 *Phys. Rev.* E **64**, 036608 (1–10) (Erratum, 2002 *Phys. Rev.* E **65**, 019904).
[4] Varma, R. K. 2003 *Phys. Reports* **378**, 301.
[5] Varma, R. K. 2007 *Pramana – J. Phys.* **68**, 901.
[6] Varma, R. K. (in press) *Pramana – J. Phys.*
[7] Varma, R. K. and Punithavelu, A. M. 1993 *Mod. Phys. Lett.* A **8**, 167.
[8] Varma, R. K., Punithavelu, A. M. and Banerjee, S. B. 2002 *Phys. Rev.* E **65**, 026503 (1–9).
[9] Varma, R. K. and Banerjee, S. B. 2007 *Phys. Scripta* **75**, 19.
[10] Ito, A. and Yoshida, Z. 2001 *Phys. Rev.* E **63**, 026502 (1–5).
[11] Varma, R. K., Punithavelu, A. M. and Banerjee, S. B. 2004 *Phys. Rev.* E **70**, 028502.